

# Strongly interacting $\sigma$ -electrons and $\text{MgB}_2$ superconductivity

V. A. Ivanov, M. van den Broek and F. M. Peeters  
 Departement Natuurkunde, Universiteit Antwerpen (UIA),  
 Universiteitsplein 1, B-2610 Antwerpen, Belgium

25th April 2001

## Abstract

$\text{MgB}(p^{n_\sigma} p^{n_\pi})_2$  is classified as a system with strongly interacting  $\sigma$ -electrons and non-correlated  $\pi$ -electrons of boron ions. The kinematic and Coulomb interaction  $V$  between the orbitally degenerated  $\sigma$ -electrons provide the superconducting state with an anisotropic gap of  $s^*$ -wave symmetry. The critical temperature  $T_c$  has a non-monotonic dependence on the distance  $r$  between the centers of gravity of  $\sigma$ - and  $\pi$ -bands.  $\text{MgB}_2$  corresponds to  $r = 0.085$  eV and  $V = 0.45$  eV in our model with flat bands. The derived superconducting density of electronic states is in good agreement with available experimental and theoretical data. The possibilities for increasing  $T_c$  are discussed.

Keywords: A. Superconductors; C. Crystal structure and symmetry; D. Electronic band structure; D. Electron correlations

The unprecedented discovery of superconductivity in the simple binary material  $\text{MgB}_2$  [1] has opened up new avenues to attack the problem of maximizing  $T_c$  and the symmetry of the order parameter. In the present paper we present a model to explain the superconducting state in  $\text{MgB}_2$  which is based on the correlated  $\sigma$ - and the non-correlated  $\pi$ -band. The negatively charged boron layers and the positively charged magnesium layers provide a lowering of the  $\pi$ -band with respect to the  $\sigma$ -band, as pointed out in Ref. [2] and which was also noticed first in band calculations [3, 4, 5]. Tight-binding estimates show that the bonding  $\sigma$ -band, close to the Fermi level, is doubly degenerate (it has  $E$ -symmetry [6, 7]). The quasi-2D  $\sigma$ -electrons are more localized than the 3D  $\pi$ -electrons. This leads to an enhancement of the on-site electron correlations in the system of degenerated  $\sigma$ -electrons. They are taken to be infinite, while the somewhat weaker intersite Coulomb interactions and electron-phonon interactions simply shift the on-site electron energies. After carrying out a fermion mapping to  $X$ -operators the Hamiltonian becomes:

$$\begin{aligned}
 H = & \sum_{p,s} t^{(\sigma)}(p) X^{so}(p) X^{os}(p) + V \sum_{\langle i,j \rangle} n_\sigma(i) n_\sigma(j) - r \sum_i n_\pi(i) + \\
 & + \sum_{p,s} \varepsilon_0^{(\pi)}(p) [\pi_s^+(p) \pi_s(p) + H.c.] - \mu \sum_i [n_\sigma(i) + n_\pi(i)]. \quad (1)
 \end{aligned}$$

It is written in the usual notations, where the non-diagonal  $X$ -operators describe the on-site transitions of correlated  $\sigma$ -electrons between the one-particle ground states (with spin projection  $s = \pm$ ) and the empty polar electronic states (0) of the boron sites and  $\mu$  is the chemical potential. The wide  $\pi$ -band is shifted with respect to the  $\sigma$ -band by an energy  $r$ . This parameter comprises the mean-field  $\pi$ -electron interactions, the electron-phonon interactions (e.g. the contribution of the strong coupling of  $E_{2g}$ -phonons with the  $\sigma$ -electrons [8]) *etc.* We included in Eq. (1) also the nearest neighbour Coulomb repulsion  $V$  of  $\sigma$ -electrons, which is essential for the low density of hole-carriers present in MgB<sub>2</sub>. The mutual hopping between  $\sigma$ - and  $\pi$ -electrons is assumed to be negligible due to the characteristic space symmetry of the orbitals involved. A schematic view of our model is presented in Fig. 1. The diagonal  $X$ -operators ( $X \equiv X^{\cdot}$ ) conform to the completeness relation,  $X^0 + 4X^s = 1$ , and their thermodynamic averages ( $\langle X^0 \rangle$ ,  $\langle X^s \rangle$ ) are the Boltzmann populations of the energy levels of the unperturbed on-site Hamiltonian in (1). Due to the orbital and spin degeneracy the  $\sigma$ -electrons occupy their one-particle ground state with density  $n_\sigma = 4 \langle X^s \rangle$  per boron site. The correlation factor for the degenerated  $\sigma$ -electrons is

$$f = \langle X^0 + X^s \rangle = 1 - 3 \langle X^s \rangle = 1 - \frac{3}{4} n_\sigma, \quad (2)$$

and it plays an important role in all arithmetics starting from their unperturbed (zeroth order) Green's function,  $D_\sigma^{(0)}(\omega) = f / (-i\omega_n - \mu)$ , whereas for  $\pi$ -electrons  $D_\pi^{(0)}(\omega) = 1 / (-i\omega_n - \mu - r)$ . Note that for the conventional Hubbard model the correlation factor in the paramagnetic phase is  $1 - n/2$  (see [9] and Refs. therein). The energy dispersion of both bands,  $\xi(p) = ft(p) - \mu$  and  $\varepsilon(p) = \varepsilon_0(p) - r - \mu$ , are governed by zeros of the inverse Green's function

$$D^{-1}(\omega, p) = \text{diag} \{ D_\sigma^{-1}(\omega, p); D_\pi^{-1}(\omega, p) \} = \text{diag} \left\{ \frac{-i\omega_n + \xi(p)}{f}; -i\omega_n + \varepsilon(p) \right\},$$

which follows from the Dyson equation

$$D^{-1}(\omega, p) = D^{(0)-1}(\omega) + \hat{t}(p),$$

to first order with respect to the tunneling matrix  $\hat{t}(p) = \text{diag}\{t(p); \varepsilon_0(p)\}$ , where  $\text{diag}\{A; B\} = \begin{pmatrix} A & 0 \\ 0 & B \end{pmatrix}$ .

The chemical potential  $\mu$  for the MgB<sub>2</sub> = Mg<sup>++</sup>B<sup>-</sup>( $p^2$ )<sub>2</sub> = Mg<sup>++</sup>B<sup>-</sup>( $p^{n_\sigma} p^{n_\pi}$ )<sub>2</sub>-system (Eq. (1)) obeys the equation for the total electron density per boron site

$$n_\sigma + n_\pi = 2, \quad (3)$$

with the partial electron densities given by

$$n_{\sigma,\pi} = 2T \sum_{n,p} e^{i\omega\delta} D_{\sigma,\pi}(\omega, p) \equiv n_{\sigma,\pi}(r, \mu). \quad (4)$$

The electron densities, Eq. (4), comply with the requirements  $0 < n_\sigma < 1$  (due to the correlation factor, Eq. (2), providing the quarter-fold narrowing of the

degenerate  $\sigma$ -band) and  $0 < n_\pi < 2$ . For any energy difference  $r$  between the  $\sigma$ - and  $\pi$ -bands the chemical potential  $\mu$  has to be such that Eq. (3) for the band fillings is satisfied.

From the system of Eqs. (3, 4) for a flat density of electronic states (DOS hereafter)  $\rho_{\sigma,\pi}(\varepsilon) = (1/2w_{1,2})\theta(w_{1,2}^2 - \varepsilon^2)$  with half-bandwidths  $w_1$  and  $w_2$  for  $\sigma$ - and  $\pi$ -electrons, respectively and  $\theta(x)$  is the theta function) we derive the chemical potential of the  $A^{2+}B(p^{n_\sigma}p^{n_\pi})_2$  systems as

$$\mu = \frac{w_2 - 5r}{5w_1 + 4w_2}w_1. \quad (5)$$

The non-correlated  $\pi$ -electrons play the role of a reservoir for the  $\sigma$ -electrons. In the energy dispersion  $\xi(p)$  for the  $\sigma$ -electrons, the correlation factor, Eq. (2), can be expressed also via the electron structure parameters  $w_1, w_2$  and  $r$  as  $f = (2w_1 + w_2 + 3r) / (5w_1 + 4w_2)$ .

The anomalous self-energy for the  $\sigma$ -electrons (Fig. 2) is written self-consistently as

$$\check{\Sigma}(p) = T \sum_{n,q} \Gamma_0(p,q) \frac{\check{\Sigma}(q)}{\omega_n^2 + \xi^2(q) + \check{\Sigma}(q)}, \quad (6)$$

where the vertex  $\Gamma_0$  is determined by the amplitudes of the kinematic and Coulomb interactions such that  $\Gamma_0(p,q) = -2t_q + V(p-q)$ . We do not include the other kinematic vertices in  $\Gamma_0$  essential for a comparative analysis of the anisotropic singlet and for triplet pairings and the energy band renormalization at a moderate concentration of carriers [9]. In momentum space the Coulomb repulsion between the nearest neighbours (Eq. (1)) reflects the tight-binding symmetry of the boron honeycomb lattice,  $\sqrt{3 + 2\left(\cos p_y + 2\cos\frac{p_x}{2}\cos\frac{\sqrt{3}p_x}{2}\right)}$ . Near the  $\Gamma - A$  line of the Brillouin zone the Coulomb vertex can be factorized as

$$V(p-q) = 2\beta t(p)t(q),$$

where the parameter  $\beta = V/6t^2$  expresses the Coulomb repulsion for the nearest  $\sigma$ -electrons and the energy dispersion is  $t(p) = 3t\left(1 - \frac{p_x^2 + p_y^2}{12}\right)$ . Putting the explicit form of the vertex  $\Gamma_0$  in Eq. (6), and after summation over the Matsubara frequencies  $\omega_n = (2n+1)\pi T$  one obtains

$$\check{\Sigma}(p) = \sum_q t(q)(1 - \beta t(p)) \check{\Sigma}(q) \frac{\tanh\sqrt{\xi^2(q) + \check{\Sigma}^2(q)}/2T}{\sqrt{\xi^2(q) + \check{\Sigma}^2(q)}}. \quad (7)$$

The search for a solution in the form  $\check{\Sigma}(p) = \Sigma_0 + t(p)\Sigma_1$  converts Eq. (7) for the superconducting critical temperature and the gap in  $A^{2+}B_2^-$  to

$$1 = \sum_p t(p)(1 - \beta t(p)) \frac{\tanh\sqrt{\xi^2(p) + \Sigma^2(p)}/2T}{\sqrt{\xi^2(p) + \Sigma^2(p)}}, \quad (8)$$

with the gap function  $\Sigma(p) = [1 - \beta t(p)]\Sigma_0$ .

Equalizing the gap function in Eq. (8) to zero, one can derive analytically  $T_c$  in the logarithmic approximation for a flat DOS :

$$T_c = \frac{w_1}{5w_1 + 4w_2} \sqrt{(w_1 + w_2 - r)(w_1 + 4r)} \exp\left(-\frac{1}{\lambda}\right),$$

$$\lambda = \frac{(5w_1 + 4w_2)(3 + 5\beta w_1)}{(2w_1 + w_2 + 3r)^3} (w_2 - 5r) \left[ r - \frac{\beta w_1 w_2 - 2w_1 - w_2}{3 + 5\beta w_1} \right]. \quad (9)$$

Under the prefactor in the square root the restrictions for an energy shift  $r$  guarantee the assumed volume of the correlated  $\sigma$ -band, namely  $n_\sigma \geq 0$  ( $r \leq w_1 + w_2$ ) and  $n_\sigma \leq 1$  ( $r \geq -w_1/4 = -t$ ).  $T_c(r)$  is plotted in Fig. 3 for different values of the parameter  $\beta$ , reflecting the suppression of superconductivity with an increase of the Coulomb repulsion. The critical temperature  $T_c$  has a non-monotonic dependence on the mutual position  $r$  of the  $\sigma$ - and  $\pi$ -bands. The MgB<sub>2</sub> case,  $T_c = 40$  K, corresponds to  $r = 0.085$  eV and a dimensionless value  $\beta w_1 = 8 \text{ V}/3w_1$ .

The superconducting gap equation follows from Eq. (8) taken for  $T=0$

$$1 = \int \rho_\sigma(\varepsilon) \varepsilon (1 - \beta\varepsilon) \frac{d\varepsilon}{\sqrt{\varepsilon^2(\varepsilon) + \Sigma_0^2(1 - \beta\varepsilon)^2}}. \quad (10)$$

It defines the anisotropic superconducting order parameter of  $s^*$ -wave symmetry. In contrast to the isotropic  $s$ -wave gap, the superconducting gap does not coincide with the amplitude  $\Sigma_0$  of the gap function and it should be defined by the minimal square root in Eq. (10).

The near-cylindrical hole-like  $\sigma$ -Fermi surfaces in MgB<sub>2</sub> gives room to calculate the superconducting DOS  $\rho(E) = \sum_p \delta\left(E - \sqrt{\varepsilon^2(p) + \Sigma^2(p)}\right)$ , where the gap function (cf. Eq. (10)) is

$$\Sigma = \Sigma_0(1 - \beta t(p)) = b(1 + a \cos^2 \vartheta), \quad (11)$$

where  $a = \beta w_1 / (12(1 - \beta w_1))$ ,  $b = \Sigma_0(1 - \beta w_1)$  and  $\vartheta$  is the azimuthal angle. Then the superconducting DOS normalized with respect to the normal DOS is

$$\frac{\rho(E)}{\rho_0(E)} = E \int_0^1 \frac{dz}{\sqrt{E^2 - b^2(1 + az^2)^2}}. \quad (12)$$

For a Coulomb repulsion such that  $\beta w_1 < 1$  the parameter satisfies  $a > 0$  and the superconducting DOS becomes

$$\frac{\rho(b < E < (1 + a)b)}{\rho_0(E)} = \sqrt{\frac{E}{2ab}} K(q),$$

$$\frac{\rho(E > (1 + a)b)}{\rho_0(E)} = \sqrt{\frac{E}{2ab}} F\left(\sin^{-1} \sqrt{\frac{ab}{(E + (1 + a)b)q^2}}; q\right), \quad (13)$$

which is expressed in terms of the complete and incomplete elliptic integrals  $K$  and  $F$ , respectively with modulus  $q = \sqrt{(E - b)/2E}$ . The DOS (13) has cusps at  $E = \pm(1 + a)b$ . A similar result was obtained in Ref. [10] for a non-specified

parameter  $a > 0$ . In our case the parameter  $a$  is controlled by the in-plane Coulomb repulsion  $V$  as the authors of Ref. [6] noted. At  $\beta w_1 = 0.92$  the DOS of Eq. (13) (see Fig. 4, inset) reproduces Fig. 1(b) of Ref. [10].

But for our case of an enhanced Coulomb repulsion  $\beta w_1 > 1$ , we have to take the parameter  $a < 0$  in the gap function (11) and the superconducting DOS (Fig. 4) is then given by

$$\begin{aligned} \frac{\rho((1-|a|)b < E < b)}{\rho_0(E)} &= \frac{E}{\sqrt{(E+b)|a|b}} F\left(\sin^{-1} \frac{1}{q}; \sqrt{\frac{2E}{E+b}}\right), \\ \frac{\rho(E > b)}{\rho_0(E)} &= \sqrt{\frac{E}{2|a|b}} F\left(\sin^{-1} q; \sqrt{\frac{E+b}{2E}}\right). \end{aligned} \quad (14)$$

For our  $a < 0$  case the superconducting DOS (14) contains two logarithmic divergencies at  $E = \pm b$  and a gap in the energy range  $|E| < (1-|a|)b$ . The "gap" ratio is  $1/(1-|a|)$ .

Measurements on MgB<sub>2</sub> with scanning tunneling spectroscopy [11, 12] and with high-resolution photo-emission spectroscopy [13] revealed the presence of these two gap sizes. From the ratio 3.3 between the two gaps in Ref. [11] we can extract the parameters  $|a| \approx 2/3$  and  $\beta w_1 \approx 1.14$  (see Eq. (11)), whereas from data of Ref. [12] one can derive  $\beta w_1 = 1.21$ . A value  $\beta w_1 = 1.14$  can be estimated from Ref. [13]. Point-contact spectroscopy [14] shows gaps at 2.8 and 7 meV, from which we estimate a Coulomb repulsion parameter  $\beta w_1 = 1.16$ . The recent study of energy gaps in superconducting MgB<sub>2</sub> by specific-heat measurements revealed "gaps" at 2.0 meV and 7.3 meV [15] for which  $\beta w_1 = 1.13$ , and a gap ratio  $3 - 2.2$  [16], for which  $\beta w_1 = 1.14 - 1.15$ . Measurements of the specific heat of Mg<sup>11</sup>B<sub>2</sub> also give evidence for a second energy gap [17]. It is worth noticing that earlier Raman measurements [18] have revealed the presence not only of the discussed peak at  $110 \text{ cm}^{-1}$ , but also of an asymmetric peak at  $65 - 60 \text{ cm}^{-1}$  (see Figs. 1 and 2 in Ref. [18]). These results correspond to a gap ratio  $0.6 - 0.54$ , from which we estimate  $|a| = 0.41 - 0.45$  (cf. Eq. (14)) and a Coulomb parameter  $\beta w_1 = 1.25 - 1.22$  (Eq. (11)). Later Raman measurements [19] established pronounced peaks, corresponding with gaps at  $100 \text{ cm}^{-1}$  and  $44 \text{ cm}^{-1}$ . From these data one can extract  $a = -0.56$  and  $\beta w_1 = 1.18$ . At  $\beta w_1 = 1$  we have gapless like superconductivity. In this case the superconducting DOS is linear with respect to the energy near the nodes of the superconducting order parameter. Then the superconducting specific heat  $C_e \sim T^2$  and the NMR boron relaxation rate  $\sim T^3$  at low temperatures (for BEDT-TTF organic salts this is shown in Ref. [20]). From this point of view it is interesting that the data of Ref. [21] shows a  $C_e \sim T^2$  behaviour and a deviation from the exponential BCS behaviour in  $T_1^{-1}(T)$  of <sup>11</sup>B [22] visualized in MgB<sub>2</sub>.

In summary, we have analyzed the superconducting properties of the material MgB<sub>2</sub> within the framework of a correlated model (1). The existing electron-phonon and non-phonon approaches to the superconducting mechanism in MgB<sub>2</sub> can be separated in two groups: one pays attention to the  $\sigma$ -electrons and the other to the  $\pi$ -electron subsystem. We have taken into account both the correlated  $\sigma$ - and noncorrelated  $\pi$ -electrons. Analysis of our results leads to the conclusion that superconductivity occurs in the subsystem of  $\sigma$ -electrons with degenerate narrow energy bands whereas the wide-band  $\pi$ -electrons play

the role of a reservoir. Superconductivity is driven by a non-phonon kinematic interaction in the  $\sigma$ -band. A lot of evidences in favour of two different superconducting gaps can be explained by anisotropic superconductivity with an order parameter of  $s^*$ -wave symmetry, induced by the in-plane Coulomb repulsion. For an enhanced interboron Coulomb repulsion ( $\beta w_1 > 1$ ) the logarithmic divergencies in the superconducting DOS (Eq. 14, Fig. 4) are manifested by a second gap in the experiments. The kinematic mechanism of superconductivity for correlated electrons was first proposed for high- $T_c$ -cuprates ([23], see [9] and Refs. therein) as a non-phonon mechanism with correlated hopping ([24], and Refs. therein). In Ref. [25] it was shown that in the strongly correlated limiting case the kinematic mechanism reproduces the result of hole dressed superconductivity. In our approach the electron-phonon coupling is hidden in the parameter  $r$ . Therefore the pressure and isotope effects can be explained by the dependence of  $r(\omega)$  on the phonon modes. From the non-monotonic  $T_c$  dependence on  $r$  it follows that the MgB<sub>2</sub> material is in the underdoped regime (around  $r \gtrsim -w_1/4$ ). For a fictitious system A<sup>2+</sup>B<sub>2</sub><sup>-</sup>, where the two electrons are contributed by atom A, the superconducting critical temperature increases with an  $r$  increase. A pressure increase lowers the  $\sigma$ -band with an  $r$  decrease resulting in a negative pressure derivative of  $T_c$  in agreement with experiment [26]. The bell shaped curve  $T_c(r)$ , with the MgB<sub>2</sub> position in the underdoped regime, shows a possibility to reach higher  $T_c$ 's in diboride materials such as A<sup>2+</sup>B<sub>2</sub><sup>-</sup> with an AlB<sub>2</sub> crystal structure. We suggest the synthesis of materials with increased  $r$ -values (e.g. with "negative chemical pressure") and optimized smaller interatomic B-B distances in the honeycomb plane.

## Acknowledgments

This work was supported by the Flemish Science Foundation (FWO-VI), the Concerted Action program (GOA) and the Inter-University Attraction Poles (IUAP-IV) research program. V. A. I. acknowledges useful discussions with K. Maki and S. Haas for sending their recent preprint.

## References

- [1] J. Nagamatsu, N. Nakagawa, T. Muranaka, Y. Zenitani, J. Akimitsu, Nature (London) 410, 63 (2001).
- [2] J. M. An, W. E. Pickett, Phys. Rev. Lett. 86, 4366 (2001).
- [3] D. R. Armstrong, P. G. Perkins, J. Chem. Soc. Faraday II 75, 12 (1979).
- [4] N. I. Medvedeva, J. E. Medvedeva, A. L. Ivanovskii, V. G. Zubkov, A. J. Freeman, JETP Lett. 73, 336 (2001)
- [5] J. Kortus, I. I. Mazin, K. D. Belashchenko, V. P. Antropov, L. L. Boyer, Phys. Rev. Lett. 86, 4656 (2001).
- [6] K. Voelker, V. I. Anisimov, T. M. Rice, cond-mat/0103082.
- [7] Y. Kong, O. V. Dolgov, O. Jepsen, O. K. Andersen, Phys. Rev. B 64, R020501 (2001).

- [8] T. Yildirim, O. Gulseren, J. W. Lynn, C. M. Brown, T. J. Udovic, H. Z. Qing, N. Rogado, K. A. Regan, M. A. Hayward, J.S. Slusky, T. He, M. K. Haas, P. Khalifah, K. Inumaru, R. J. Cava, Phys. Rev. Lett. 87, 37001 (2001).
- [9] V. Ivanov, Europhys. Lett. 52, 351 (2000).
- [10] S. Haas, K. Maki, cond-mat/0104207; preprint.
- [11] C.-T. Chen, P. Seneor, N.-C. Yeh, R. P. Vasquez, C. U. Jung, Min-Seok Park, Heon-Jung Kim, W. N. Kang, Sung-Ik Lee, cond-mat/0104285.
- [12] F. Giubileo, D. Roditchev, W. Sacks, R. Lamy, D. X. Thanh, J. Klein, S. Miraglia, D. Fruchart, J. Marcus, Ph. Monod, cond-mat/0105592.
- [13] S. Tsuda, T. Yokoya, T. Kiss, Y. Takano, K. Togano, H. Kitou, H. Ihara, S. Shin, cond-mat/0104489.
- [14] P. Szabo, P. Samuely, J. Kacmarcik, Th. Klein, J. Marcus, D. Fruchart, S. Miraglia, C. Marcenat, A. G. M. Jansen, cond-mat/0105598.
- [15] R. A. Fisher, F. Bouquet, N. E. Phillips, D. G. Hinks, J. D. Jorgensen, cond-mat/0107072.
- [16] A. Junod, Y. Wang, F. Bouquet, P. Toulemonde, to appear in: A. Marlikov (Eds.), Studies of High Temperature Superconductors, Vol. 38, Nova Science, New York; cond-mat/0106394.
- [17] F. Bouquet, R. A. Fisher, N. E. Phillips, D. G. Hinks, J. D. Jorgensen, Phys. Rev. Lett. 87, 047001 (2001)
- [18] X. K. Chen, M. J. Konstantinovic, J. C. Irwin, D. D. Lawrie, J. P. Franck, cond-mat/0104005 version 1 (31 March 2001).
- [19] X. K. Chen, M. J. Konstantinovic, J. C. Irwin, D. D. Lawrie, J. P. Franck, cond-mat/0104005 version 2 (21 May 2001).
- [20] V. A. Ivanov, E. A. Ugolkova, M. Ye. Zhuravlev, JETP 86 (1998) 395.
- [21] Y. Wang, T. Plackowski, A. Junod, Physica C 355, 179 (2001).
- [22] A. Gerashenko, K. Mikhalev, S. Verkhovskii, T. D'yachkova, A. Tyutyunik, V. Zubkov, cond-mat/0102421.
- [23] R. O. Zaitsev, V. A. Ivanov, Sov. Phys. Solid State 29, 1475, 1784 (1987); JETP Lett. 46, 140 (1987); V. A. Ivanov, R. O. Zaitsev, Intern J. Mod. Phys. B 1, 689 (1988), *ibid.* 3, 1403 (1989).
- [24] J.E. Hirsch, Phys. Lett. A 282, 392 (2001).
- [25] V. A. Ivanov, M. Ye. Zhuravlev, Theor. and Mathem. Physics 86, 215 (1991); Physica C 185, 1587 (1991).
- [26] H. Tou, T. Takenobu, T. Ito, Y. Iwasa, K. Prassides, T. Arima, J. Phys.: Condens. Matter 13, L267 (2001).

## Figure captions

**Fig. 1** A schematic view of the energy band diagram. The degenerate  $\sigma$ -electrons are represented by a lower correlated band.

**Fig. 2** The anomalous self-energy  $\check{\Sigma}(p)$  for  $\sigma$ -electrons. The solid line is an anomalous Green's function (cf. Eq. (6)).

**Fig. 3** The non-monotonic dependence of  $T_c(r)$  at different magnitudes of the Coulomb repulsion (parameter  $\beta w_1$ ). Here  $w_2/w_1 = 8$ . MgB<sub>2</sub> is marked in the inset with a solid circle positioned at  $r = 0.085$  eV and  $\beta w_1 = 1.2$  for  $w_1 = 1$  eV and  $w_2 = 8$  eV.

**Fig. 4** The superconducting DOS, normalized with respect to the normal DOS, for the Coulomb parameter range  $\beta w_1 > 1$ . At  $\beta w_1 = 0.92$ , the Maki result [10] is reproduced (inset) (cf. Eq. (13)).

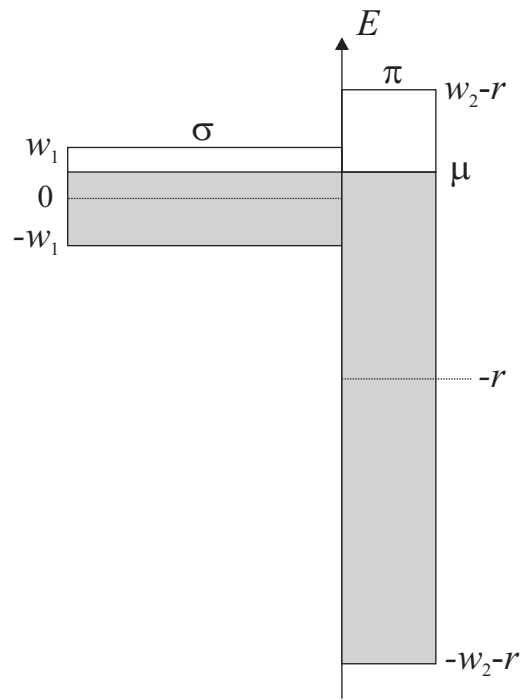


Fig. 1: Ivanov et al.

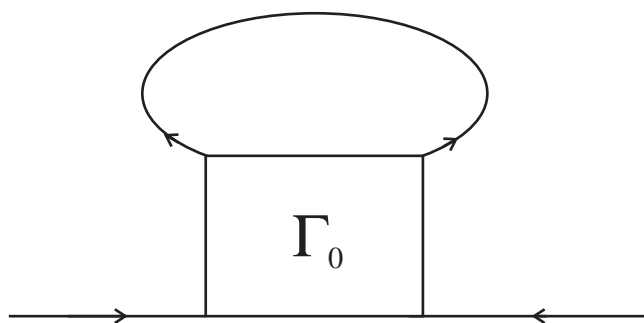


Fig. 2: Ivanov et al.

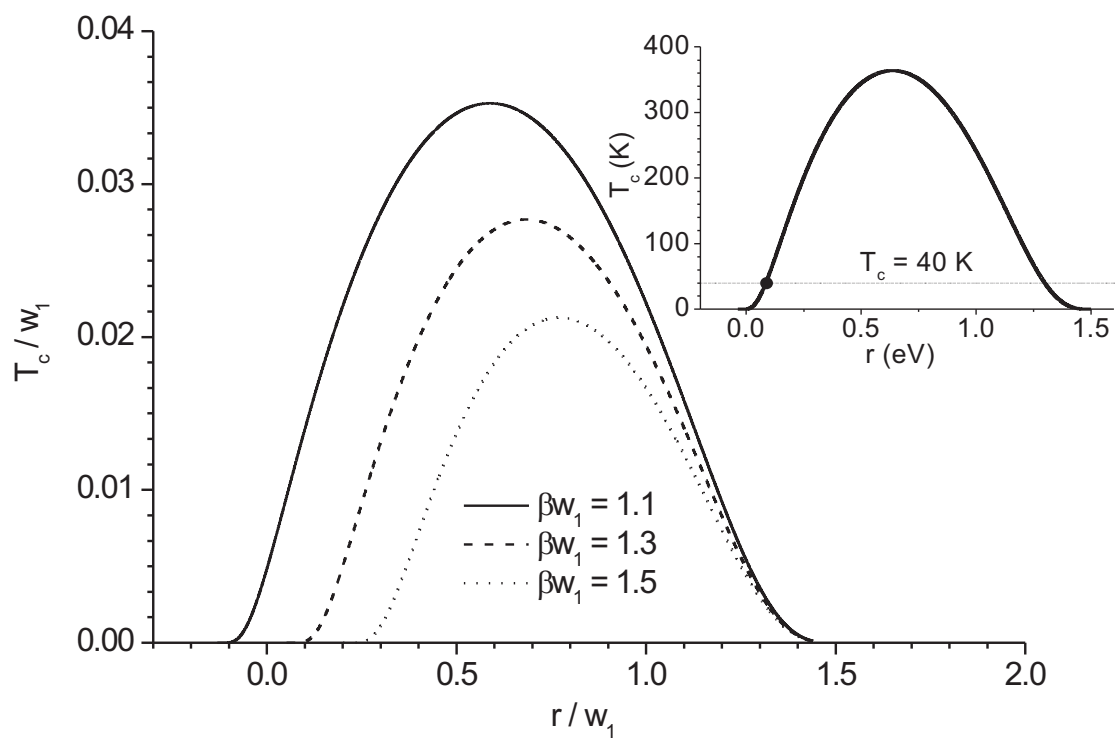


Fig. 3: Ivanov et al.

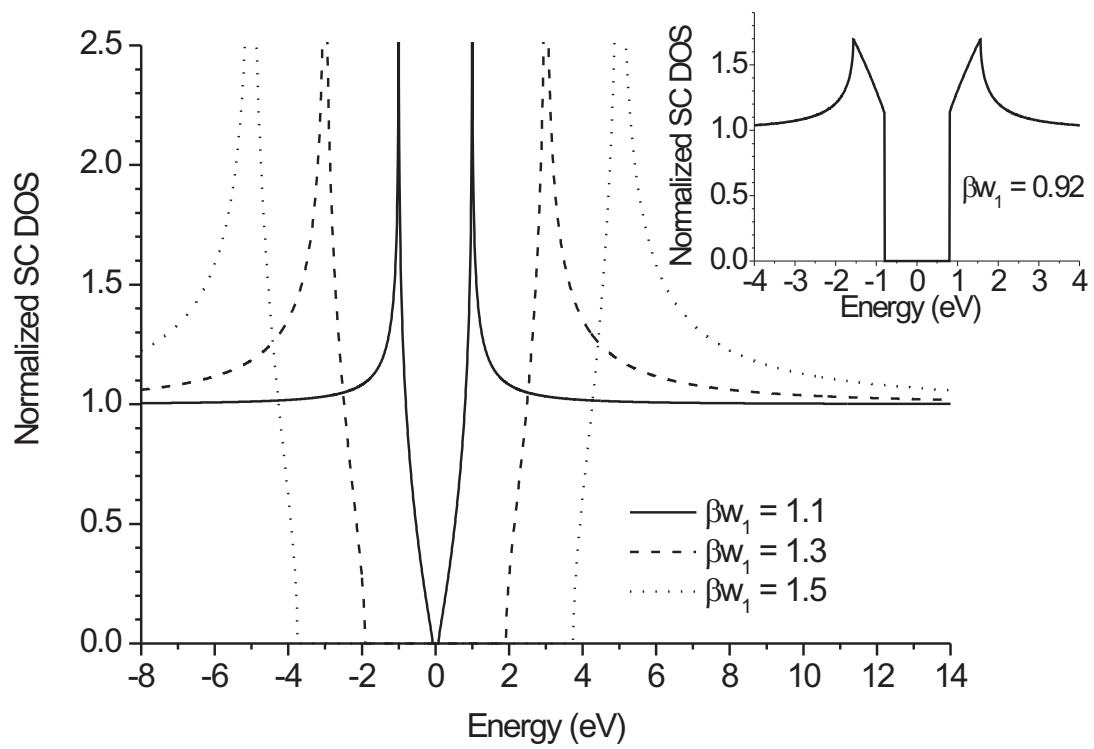


Fig. 4: Ivanov et al.